The non-specific Lipid Transfer Protein (nsLTP) is involved at early and late stages of symbiosis between *Alnus glutinosa* and *Frankia alni*.

Mélanie GASSER[1], Nicole ALLOISIO[1], Pascale FOURNIER[1], Severine BALMAND[2], Ons KHARRAT[1], Joris TULUMELLO[1,3], Abdelaziz HEDDI[2], Pedro Da SILVA[2], Philippe NORMAND[1], Hasna BOUBAKRI[1#], Petar PUJIC[1]

1-Université de Lyon, F-69361, Lyon, France ; Université Claude Bernard Lyon 1, CNRS, UMR 5557, INRAE UMR1418, Ecologie Microbienne, F-69622, Villeurbanne, France

2-INSA-Lyon, INRAE, UMR203 BF2i, Biologie Fonctionnelle Insectes et Interactions, Villeurbanne, France

3-present address: Aix Marseille Univ, CEA, CNRS, BIAM, Lab Microbial Ecology of the Rhizosphere (LEMiRE), F-13108, Saint-Paul-Lez-Durance, France; BioIntrant 139, Rue Philippe de Girard, Pertuis F-84120, France.

#corresponding author: hasna.boubakri@univ-lyon1.fr, tel: 33-472 44 82 00

Summary

Alnus glutinosa response to *Frankia alni* is driven by several sequential physiological modifications that include calcium spiking, root hair deformation, penetration, induction of primordium, formation and growth of nodule. Here, we have conducted a transcriptomic study to analyse plant responses to *Frankia alni* at early stages of symbiosis establishment.

Forty-two genes were significantly activated by either with a *Frankia* culture supernatant or with living cells separated from the roots by a dialysis membrane

permitted to identify plant genes which expression changes upon early contact with *Frankia*. Most of these genes encode biological processes, including oxidative stress and response to stimuli. The most upregulated gene is the non-specific lipid transfer protein (nsLTP) encoding gene with a fold change of 141. Physiological experiments showed that nsLTP increases *Frankia* nitrogen fixation at sub-lethal concentration. Immunohistochemistry experiments conducted at an early infection stage indicated that nsLTP protein is localized at the deformed root hair region after *Frankia* inoculation and later in nodules, precisely around bacterial vesicles. Taken together, these results suggest that nsLTP acts at early and late stages of symbiosis, probably by increasing nitrogen uptake by *Frankia*.

Keywords: nitrogen fixation, antimicrobial peptide, immunity, root hairs, oxidative stress, lipid, infection threads, nodule

Introduction

Symbiosis between *Alnus glutinosa* and the actinobacterium *Frankia alni* permits the establishment of root nodules in which nitrogen fixation takes place. This helps alder and other plants collectively called "actinorhizal" to grow on nitrogen-poor soils and initiate ecological successions. The determinants of this interaction are poorly known, due among other reasons to the lack of a transformation system in alder. *Alnus glutinosa* is the type species of the genus (Navarro *et al.*, 2003), it grows in pioneer biotopes such as glacial moraines, volcanic ashes and mine spoils (Normand & Fernandez, 2019) and its genome has been deciphered recently (Griesmann *et al.*, 2018).

The presence of a symbiotic bacterium like *Frankia* or simply that of its exudates, triggers in the host plant tissues a series a events leading to root hair deformation and

51 calcium spiking (Granqvist *et al.*, 2015). Later, penetration, primordium formation and
52 growth of nodules follow with subsequent exchange of nutrients. Omic analyses have
53 permitted to gain a global view of the physiological changes taking place upon specific
54 challenges. In particular, transcriptomics of 21 day post-inoculation (dpi) nodules
55 permitted to see on the plant side the presence of homologs of the whole common
56 symbiotic signalling cascade or CSSP (Hocher, V. *et al.*, 2011; Hocher, Valérie *et al.*,
57 2011), some of which have been lost in non-symbiotic neighbours (Griesmann *et al.*,
58 2018).
59 This important conservation on the plant side of the common symbiotic pathway
60 (Hocher, V. *et al.*, 2011) contrasts with the absence in most *Frankia* genomes (Normand
61 *et al.*, 2007) of the canonical *nod* genes which are involved in the biosynthesis of Nod
62 Factor (NF) in majority of Rhizobia (D'Haeze & Holsters, 2002). In mature nodules, the
63 bacterial genes *nif, hup, shc* and *suf* are upregulated but no trace of a symbiotic island
64 was found (Alloisio *et al.*, 2010). A study of the *Frankia alni* early response (2.5 dpi)
65 showed that several determinants were upregulated among which a K-transporter, lipid
66 modifying enzymes and a conserved cellulose synthase cluster (Pujic *et al.*, 2019).
67 Proteomics was performed on a related species, *Frankia coriariae* that unravelled an
68 upregulation of cell wall remodelling enzymes, signal transduction and host signal
69 processing proteins (Ktari *et al.*, 2017). Metabolomics on an *Alnus*-infective strain
70 showed the presence of various compounds absent from roots (Hay *et al.*, 2017), high
71 levels of TCA intermediates citrate, fumarate and malate (Carro *et al.*, 2015a) and high
72 levels of citrulline, glutamate and pyruvate (Brooks & Benson, 2016; Hay *et al.*, 2020).
73 Signalling between alder and *Frankia alni* involves on the part of the bacterium the
74 synthesis of an uncharacterized root hair deforming factor (Ghelue *et al.*, 1997;
75 Cérémonie *et al.*, 1999) and that of the auxin PAA (Hammad *et al.*, 2003). On the plant

76 side, less is known besides the upregulation of defensins that modify the porosity of
77 *Frankia* membranes (Carro *et al.*, 2015b; Carro *et al.*, 2016).
78 We undertook the present study to better understand the initial steps of the actinorhizal
79 symbiosis on the plant side where the symbiont must be recognized to pave the way for
80 its internalization. To analyse this early plant responses to *Frankia* symbiont we have
81 conducted a cell-free contact through two conditions: indirect contact with *Frankia*
82 trapped in dialysis tube or its supernatant and by targeting 2.5 dpi response, by which
83 time extensive root hair deformation has occurred (Berry & Torrey, 1983) and before
84 primordium formation at 7dpi (Lalonde, 1979). We further focussed on the most
85 upregulated gene coding a non-specific Lipid Transfer Protein (nsLTP), which is also one
86 of the most overexpressed genes in the nodule. We showed that nsLTP increases *Frankia*
87 nitrogen fixation at sub-lethal concentration. Taken into account that this protein shown
88 to localize at the deformed root hairs and in *Frankia's* vesicles inside nodules, we
89 hypothesized that nsLTP acts at early and late stages of symbiosis.
90

91 **Materials and methods**

92 **Strains and growth condition before total RNA extraction**

93 Plant samples at early stages of infection were obtained as described previously(Pujic *et*
94 *al.*, 2019). Briefly, *Frankia alni* ACN14a (Normand & Lalonde, 1982) was grown in BAP-
95 PCM media until log-phase, collected by centrifugation, washed twice with sterile ultra-
96 pure water and suspended in Farhaeus medium without $KN0_3$. *Frankia* cells were
97 homogenised by forced passage through a series of needles (21G, 23G, 25G, 27G) before
98 inoculation.
99 *Alnus glutinosa* seeds obtained from a single individual growing on the banks of the river
100 Rhone in Lyon were surface sterilised and grown as described earlier (Pujic *et al.*, 2019).

101 Seedlings were transferred to Fåhraeus' solution (Fahraeus, 1957) in opaque plastic
102 pots (8 seedlings/ pot) and grown for four weeks with 0.5 $g.L^{-1}$ KNO_3, followed by one
103 week without KNO_3 before inoculation.
104 Two independent experiments were performed. In experiment #1 (Exp 1- *Frankia*
105 indirect contact (*F*IC)), 8ml of *Frankia* cells were transferred to dialysis tubing
106 (MWCO=100kDa) and arranged into a plastic pot containing 8 seedlings and filled with
107 Fåhraeus' solution without KNO_3. Five biological replicates were performed with 4
108 plastic pots per replicate. In experiment #2 (Exp2-*Frankia* supernatant direct contact
109 (SupC)), *Frankia* supernatants were applied directly on *Alnus* roots. Supernatant extract
110 was prepared as follow: 250 ml log-phase culture cells were removed by centrifugation
111 and the supernatant filtered through 0.22 µm membranes (Millipore, Billerica, MA).
112 Solid phase extractions of the supernatants were done using benzene sulphonic acid
113 cation exchanger on silica (Macherey Nagel, Hoerdt, France). Elution was done using
114 50:50 v/v methanol-water followed by 100 % methanol. Two fractions were lyophilised
115 under vacuum, dissolved in water and tested for root hair deformation activity on
116 independent plant roots. In parallel, as a control condition without supernatant, an
117 equivalent volume of culture medium was treated with the same extraction protocol.
118 Three biological replicates were performed with 6 seedlings per replicate.
119 The root hair deformation process took place similarly in both direct and indirect
120 contact conditions, confirmed with stereomicroscope observations (Leica MZ8, Wetzlar,
121 Germany). After 2.5 days (64 hours) with root hairs highly deformed, a 2 cm long
122 segment representing the central part of the root was cut at 2 cm from the distal end,
123 washed with sterile water before freezing in liquid nitrogen and storing at -80° C. In
124 addition, a T0 control condition without *Frankia* was performed and plant roots were
125 washed and frozen as described above.

126

127 **Transcriptomics of alder at 2.5dpi**

128 Transcriptomics was done as described earlier (Hocher, V. *et al.*, 2011). Total RNA was
129 purified from roots using RNeasy plant mini kits (Qiagen, Courtaboeuf, France) and
130 treated with DNases as before. Residual DNA was removed using the Turbo DNA free kit
131 (Ambion, Thermo Fisher Scientific, Wilmington, DE), quantified using a NanoDrop
132 spectrophotometer (Thermo Fischer Scientific) and qualitatively assessed using a
133 Bioanalyzer 2100 (Agilent, Waldbronn, Germany).

134 Microarrays were designed (13909 probes; 1 probe/*A. glutinosa* unigene),
135 manufactured and hybridised by Imaxio (http://www.imaxio.com/index.php), using
136 Agilent Technologies (http://www.home.agilent.com/agilent/home.jspx) as previously
137 described (Hocher, V. *et al.*, 2011). The microarrays were scanned with an Agilent
138 G2505C Scanner. The Feature Extraction software (Agilent, version 11.5.1.1) was used
139 to quantify the intensity of fluorescence signals and microarray raw data were analysed
140 using GeneSpring GX 12.0 software (Agilent technologies). Normalisation per chip (to
141 the 75th percentile) and per probe (to the median) were performed to allow comparison
142 of samples. The two experiments Exp 1 and Exp 2 were analysed separately. In order to
143 limit false positive results, microarray data were filtered according to the flag parameter
144 "detected". Thus, probes taken into account are uniform, non-outlying, non-saturated
145 and displayed an intensity level above the background in at least one of the two
146 biological conditions.

147 In Exp1, 1590 probes yielding an intensity level significantly below the background in
148 the 10 samples were discarded. In addition, 1146 probes did not yield the flag
149 "detected" in at least one of the two biological conditions and were also discarded. Thus,
150 11 173 probes were taken into account for subsequent analyses of Exp 1.

151 In Exp 2, 1765 probes yielded an intensity level significantly below the background in
152 the 6 samples and were discarded. In addition, 1113 probes did not yield the flag
153 "detected" in at least one of the two biological conditions and were also discarded. Thus,
154 11031 probes were taken into account for subsequent analyses of Exp 2. T-tests
155 comparing *F*IC roots *vs.* control roots in Exp 1 and SupC roots *vs.* control roots in Exp 2
156 were applied and only those genes with an average fold change (FC) above 2 (up-
157 regulated) or below 0.5 (down-regulated) with a p-value<0.05 were considered
158 significant. The normalized and raw microarray data values have been deposited in the
159 Gene Expression Omnibus database (www.ncbi.nlm.nih.gov/geo; accession nos. E-
160 MTAB-8936 and E-MTAB-8937).
161
162 **Quantitative real-time RT-PCR**
163 Reverse transcription (RT) and real time quantitative PCR (qRT-PCR) were performed
164 with the same biological replicates used for microarray experiments. For *A. glutinosa*
165 analyses, RT was performed with 5 µg of total mRNA using Transcriptor Reverse
166 Transcriptase and oligo $(dT)_{15}$ primer (Roche, Mannheim, Germany). QRT-PCR was run
167 on a LightCycler 480 (Roche) using LightCycler 480 SYBR Green I Master (Roche) under
168 the following conditions: 95 °C for 5 min; 45 cycles of 95 °C for 20 s, 60 °C for 20 s and
169 72 °C for 15 s. Primer sets were designed using ProbeFinder (Roche) and Primer 3
170 softwares and can be seen as Supporting Information (Table S1). Two qRT-PCR
171 reactions were run for each biological replicate and each primer set. Expression values
172 were normalised using the expression level of the *Ag-ubi* gene that encodes ubiquitin
173 (Hocher, V. *et al.*, 2011).
174
175 **Cloning of *agLTP24* gene**

176 The *agltp24* gene was PCR amplified from cDNA prepared above using designed
177 primers (Table S1) under the following conditions: 98 °C for 30 s; 30 cycles of 98 °C for 7
178 s, 63 °C for 20 s and 72 °C for 8 s. The reaction mixture of 50 µl PCR contained 1X
179 Phusion HF buffer, 200 µM dNTPs, 0.5 µM Forward primer, 0.5 µM reverse primer, 87 ng
180 template DNA and 1-units Phusion DNA Polymerase (NEB, Evry, France). The PCR
181 product was cloned using the hot fusion method (Fu *et al.*, 2014) in pET30a+ vector
182 (Merck, Molsheim France) pre-digested with *Eco*RI and *Bgl*II in order to fusion AgLTP24
183 with a N- terminal 6XHis flag. Ligation mixture was transformed in *Escherichia coli*
184 DH5α chemocompetent cells (Chung *et al.*, 1989) for plasmid DNA propagation and
185 sequencing (pET30a-HIS-AgLTP24, supplemental Fig. S1). Plasmids DNA was prepared
186 using (Nucleospin Plasmid DNA kit Macherey Nagel) from 4 independent clones, 2 ml of
187 each *E. coli* culture grown overnight in 5ml LB medium at 37°C with shaking. Cloned
188 insert DNA was checked by Sanger sequencing (Biofidal, Lyon, France) and used for
189 electrotransformation into iSHuffle T7 *lysY E. coli* cells (NEB, Evry, France), a strain used
190 to obtain proteins with disulphide bonds (Lobstein *et al.*, 2012).
191
192 **AgLTP24 production and purification**
193 Cultures were grown in LB medium supplemented with kanamycin (40µg.ml^{-1}) at 30°C
194 at 130 rpm until log phase was reached (OD_{600} ~0,5) then the HIS-AgLTP24 expression
195 was induced with 1 mM isopropyl β-D-1-thiogalactopyranoside (IPTG). Induced cultures
196 were incubated at 30°C for 3h at 130 rpm and harvested by centrifugation (5100 g for
197 10 min at 4°C). Expression was analysed by 4-20% Tricine SDS-PAGE (Schagger, 2006).
198 Pellets were lysed by freeze thaw and resuspended in a binding buffer (100 mM Tris,
199 500 mM NaCl, 5mM Imidazole, pH 7.4). A second lysis was performed using silica beads
200 and Fastprep 24™ 5G (MP Biomedicals). The cell lysate was harvested by centrifugation

201 at 5100 g, 4°C for 30min and used for the purification of HIS-AgLTP24 using His
202 GravityTrap columns (GE Healthcare) with modified binding (100mM Tris, 500mM NaCl,
203 5mM Imidazole, pH 7.4) and elution buffers (100 mM Tris, 500 Nacl, 500 mM Imidazole,
204 pH 7.4). Purification of HIS-AgLTP24 was verified by 4-20% Tricine SDS-PAGE. Elution
205 fractions was applied to a 3K MWCO Amicon Ultra-15 centrifugal filter (Merck Millipore)
206 to buffer exchange with the enterokinase buffer (20 mM Tris, 50 mM NaCl, 2 mM $CaCl_2$,
207 pH 6.8) and concentrate. The HIS tag was removed from the mature sequence of
208 AgLTP24 with enterokinase (NEB, Evry, France) for 16 h at room temperature. Cleavage
209 was confirmed by 4-20% Tricine SDS-PAGE. The enterokinase was removed from the
210 mixture using the Enterokinase Removal Kit (Sigma). His tag removal was done with a
211 His GravityTrap column (GE-Healthcare) using an imidazole free binding buffer (100
212 mM Tris, 500 mM NaCl, pH 7.4). Wash fractions containing AgLTP24 purified were
213 applied to a 3K MWCO Amicon Ultra-15 centrifugal filter (Merck Millipore) for buffer
214 exchange with NH_4^+-free FBM medium (FBM-). Final concentration was determined with
215 Qubit Protein Assay Kit (ThermoFisher). The purified AgLTP24 protein were further
216 analysed by UPLC-ESI-HRMS. The system used for UPLC-ESI-HRMS was an ultra-
217 performance liquid chromatography Ultimate 3000 (Thermo Fisher Scientific, Villebon-
218 sur-Yvette, France) coupled to a high resolution hybrid quadrupole-time of flight mass
219 spectrometer (Impact II, Bruker, Brême, Germany) equipped with electrospray
220 ionization source (ESI) (Bruker, Brême Germany). Instrument control and data
221 collection were performed using Data Analysis 5.0 software.
222
223 **Immunolocalization of AgLTP24**
224 Immunostaining and fluorescence microscopy was done as described earlier (Login *et*
225 *al.*, 2011) with the synthesised epitope (DKHSTADFEKLAPCGKAAQD) injected to a

226 rabbit (Covalab). Plant immunolocalization was performed on *A. glutinosa* roots (2.5
227 dpi) as described above in Exp 1 (*F*indC). In addition, nodules (21dpi) obtained as a
228 previous study (Carro *et al.*, 2015b) were also used here to localise agLTP24 at the
229 mature stage of symbiosis. T0 non-infected seedlings were used as control.
230
231 **Physiological assays with AgLTP24 on *Frankia alni*.**
232 The antimicrobial activity of AgLTP24 (using 1µM, 2µM, 5µM concentrations), was done
233 using the resazurin assay in 24-well microplates (Greiner bio-one, Les Ulis, France). A 2-
234 week-old *Frankia* ACN14a culture grown in FBM medium supplemented by 5mM of
235 NH_4Cl (FBM+) was centrifuged at 5100 g for 15 minutes, the supernatant was removed,
236 and the pellet homogenized in FBM- by repeated passage through syringes. *Frankia*
237 culture was done in 1ml of FBM- per well with a final optical density of 0.02 and with an
238 appropriate concentration of AgLTP24 peptide. Four replicates were made for each
239 condition. Negative (*Frankia* ACN14 in FBM-) and positive controls (*Frankia* ACN14a in
240 FBM- supplemented by kanamycin at 40µg.ml^{-1} final concentration) were performed.
241 Microplates were incubated at 28°C, 80 rpm in a humid incubator. After 6 days of
242 incubation, resazurin (Fisher Scientific SAS, Illkirch, France) was added to a final
243 concentration of 6.25µg.ml^{-1} in each well and the microplates were incubated at 28°C, 80
244 rpm for 16 hours in the dark. Fluorescence measurements were performed with a
245 microplate reader (infinite M200PRO, TECAN) with an excitation wavelength of 530nm
246 and an emission wavelength of 590nm. The results obtained were normalised to the
247 mean fluorescence of the negative control. Since data were normally distributed, mean
248 comparisons with the negative control were performed with a Student's *t*-test.
249 A second bioassay was made by growing *F. alni* in FBM- and incubating from 1 to 14
250 days at 28°C (5 replicates by kinetic point and by condition) as described previously. At

251 each kinetic point, the effects nitrogen fixation (or ARA), respiration (IRA) and on
252 morphology were monitored (Prin *et al.*, 1990; Carro *et al.*, 2015b). Since data were
253 normally distributed or not, different statistical tests were made using GraphPad Prism
254 9.2.0 (GraphPad software Inc; San Diego, CA, USA).
255
256 **Bioinformatics**
257 Blast analyses and GO assignation were performed on Blast2GO v5.2 using BLASTx
258 against NR, Gene Ontology (GOs) and Inter-ProScan (Conesa & Gotz, 2008). Fishers'
259 exact test implemented in Blast2GO was used to identify significantly enriched GO
260 categories. A GO category was considered significantly enriched only when the *p*-value
261 for that category was < 0.05 after applying FDR correction. Molecular mass of proteins
262 and their isolectric point were calculated through the Expasy software
263 (https://web.expasy.org/protparam/)
264
265
266 **Results**
267 **Transcriptomics response of alder at 2dpi**
268 In the first early response transcriptomic experiment (Exp 1), 300 and 225 genes were
269 found to be significantly up- or down- regulated in *A. glutinosa* after 2.5 days post
270 inoculation (dpi) of *Frankia* in a separated dialysis bag (cut off 100 KDa -*Frankia*
271 indirect contact (*F*indC) roots/ control roots) by having a fold change (FC) ≥ 2 or ≤ 0.5 (p
272 ≤ 0.05), respectively (Table S2). In Exp2, 248 *A. glutinosa* genes were found to be
273 significantly regulated 2.5 dpi with *Frankia* supernatant (*Frankia* supernatant contact
274 (*F*supC) roots/control roots). Of these, 176 and 76 genes were also up- and down-

275 regulated in Exp2; respectively (Table S3). By comparing ESTs present in both
276 experiments, 84 genes were found significantly up- or down-regulated (See SI Table S4).
277
278 **Biological processes implicated in early steps of symbiosis**
279 A GO-based analysis of the biological processes enriched in up- and down-regulated
280 genes within each experiment yielded 12 to 23 % of genes with no Blast hit (Fig. S2).
281 Among the sequences with a Blast hit, 8 to 14% correspond to unknown proteins and
282 could not be associated to any biological process. The annotated sequences retrieved
283 were distributed in 21 different processes (Fig. **1a**). The presence of *Frankia* at early
284 stages strongly activated genes involved in response to stimuli and catabolic processes
285 among which oxidative stress (oxidase, peroxidase) and defence (chitinase, defensin,
286 thaumatin…) were upregulated in both conditions, as well as a large portion of genes
287 involved in nitrogen compound metabolic processes with kinases, transferases, lyases or
288 glucosidases. Globally, the number of sequences retrieved was higher in Exp1 than Exp2
289 (Fig. **1a**), suggesting a stronger signal detected in indirect interaction through dialysis
290 tubing.
291 A statistical analysis permitted to identify certain enzyme families by comparing each
292 pool of genes. Even this Fisher test made in both experiment, only Exp1 gave differences
293 in GO assignation between up and down-regulated genes (Fig. **1b**).
294 In Exp1, an overrepresentation of genes coding enzymes involved in oxidation-reduction
295 biological processes and oxidative stress responses was seen with numerous
296 peroxidases, catalases, oxidases or lipoxygenases overexpressed (Table S1). Also,
297 chemical reactions involving alpha and aromatic amino acid metabolism and fatty acid
298 beta-oxidation, selenocysteine methyltransferase, phenylalanine ammonia lyase or
299 caffeic acid O-methyltransferase were seen following indirect contact with *Frankia* cells.

300 Nucleotide binding proteins such as a receptor kinase (AG-N01f_037_C05), a uridine
301 kinase (AG-N01f_030_B06) or a calcium transporting membrane (AGCL1701Contig1)
302 were also more abundant in the set of up-regulated proteins of Exp1. Finally, several
303 genes coding defence response were overrepresented such as endochitinase, disease
304 resistance protein, defensin, thaumatin, allergen or nsLTP. Conversely, we observed an
305 enrichment in down-regulated genes of one molecular function of GO assignation:
306 isomerase such as inositol-3-phosphate synthase, ribose-5-phosphate isomerase or
307 beta-amyrin synthase.
308
309 **The most upregulated genes in both experimentations**
310 By compiling differentially regulated genes found in both experiments (Table 1 and
311 Table S4), we compared them through GO-based analysis. An overrepresentation of only
312 one biological process (lipid metabolism) in down-regulated genes was found with the
313 same statistical restriction (FDR<0.05). Indeed, several genes, including synthase,
314 reductase and oxidase and involved in triterpenoid (AG-N01f_010_H21) isopentenyl
315 diphosphate (IPP) and dimethylallyl diphosphate (AG-N01f_014_J09); geranyl or
316 geranylgeranyl diphosphate (GPP and GGPP) (AG-N01f_005_E08; AG-J07f_004_F15) or
317 terpene (AG-J07f_004_M14; AGCL3086Contig1) biosynthesis were detected as more
318 abundant in down-regulated genes and already observed by our first GO assignation
319 (Fig. **1a**).
320 Amongst the 42 most upregulated genes found in both conditions (Table 1), the most
321 upregulated gene encodes a non-specific lipid transfer protein or nsLTP (fold changes:
322 140.7 (*F*indC) and 74.8 (*F*supC)), followed by a betabutilin and a pectin methylesterase
323 inhibitor. Remarkably, 20 out these 42 up-regulated genes encoded proteins with a
324 peptide signal (Table 1). Among them, numerous upregulated genes encode secreted

325 peptides (47%), some of them are classified as antimicrobial: three defensins (Ag5, Ag3
326 and Ag11), a nsLTP and a thaumatin like-protein.
327 To confirm the level of expression at this early step, we focussed on two genes, one
328 coding the nsLTP and the second coding the basic blue copper protein (fold changes:
329 (fold changes: 140.7 (*F*indC) and 74.8 (*F*supC), 4.7 (*F*indC) and 11.7 (*F*supC),
330 respectively) as candidate genes for qRT-PCR with two primer pairs per gene (Table S1).
331 Up-regulation was confirmed by qRT-PCR with the same biological replicates previously
332 used (Table S5).
333 In order to examine the temporal distribution of expression, we extracted from our
334 previous work (Hocher, V. *et al.*, 2011) the fold change obtained with the same
335 microarray but at 21 dpi when the nodule is formed and compared it to non-infected
336 roots (Table 1, Fig. 2).
337 Almost down-regulated genes at early stage were either repressed or not modulated at
338 nodule stage. Among them, we observed an enrichment of proteins associated to lipid
339 metabolic process and lyase activity. Conversely, genes upregulated at 2.5 dpi are
340 classified in three profiles. Sixteen are still induced when 17 are not modulated and 8
341 are repressed in nodule. For instance, genes encoding proteins involved in stress
342 response are found in the three profiles (Fig. 2) but we found mainly AMPs (defensin,
343 thaumatin) in the first group when chitinase and peroxidase enriched the two other
344 groups (Table 1). The nsLTP found as the most upregulated gene at early stage
345 presented also a very high expression at 21 dpi (FC=2145 in nodule, Table 1) suggesting
346 a requirement all along the symbiosis process. NsLTPs are classified as AMPs and
347 annotated as systematic acquired resistance according GO analysis suggest its potential
348 role in defense response. For all these reasons, we decided to focus our functional
349 analysis on this protein.

350

351 **Structure and classification of AgLTP24**

352 The nsLTP from *A. glutinosa* overexpressed during its interaction with *Frankia* is named
353 AgLTP24. The total nucleotide sequence is 552 base pairs and contains one exon. This
354 sequence encodes a putative processed protein of 114 amino acids including a signal
355 peptide with a sequence of 22 amino acids that allows its secretion [29]. The mature
356 peptide has a molecular weight of 9700.28 Dalton and a cationic isoelectric point of 8.46,
357 this nsLTPs is classified according to Edstam et al. (Edstam *et al.*, 2011) as Type D. It
358 contains the characteristic motif of nsLTPs composed of 8 cysteines: C-X13-C-X14CC-X9-
359 C-X1-C-X24-C-X10-C which stabilises the 3D structure by folding the α-helices domains
360 with disulphide bridges forming a hydrophobic cavity.

361

362 **Immunolocalization of AgLTP24 in planta**

363 In order to determine where this nsLTP is secreted during symbiosis establishment, we
364 performed an immunohistolocalization within plant tissues. Antibodies anti-AgLTP24
365 were applied to different alder tissues inoculated or not by *Frankia*. First, we produced
366 deformed root hairs after an indirect contact of *Frankia* (F indC) and observed signals in
367 extracellular nooks (Fig. **3b** and Fig. **3c**). These nooks were the specific site for *Frankia*
368 binding. No signal was detected with control rabbit serum (Fig. **3a**) or with anti-
369 AgLTP24 against non-infected roots (Fig. S3). Microarrays and qRT-PCR showed
370 overexpression of this protein in mature 21 dpi nodules. We observed a specific
371 immunolocalization in plant cells infected by *Frankia* situated in the fixation zone of the
372 nodule (Fig. **3e**), specifically on *Frankia's* vesicles (Fig. **3f**).

373

374 **Biological production of AgLTP24**

375 The nsLTPs are low molecular weight peptides rich in cysteines. It has a signal sequence
376 that allows the plant to address it to a target compartment. Those nsLTPs are
377 characterized by a conserved motif of 8 cysteines in their mature sequence forming 4
378 disulfide bonds important for the formation of the hydrophobic cavity, which makes
379 their production difficult. Synthetic production is limited to small peptides with few
380 disulfide bonds, so we developed a biological production of mature AgLTP24, i.e.
381 without its signal peptide, in *E. coli* shuffle T7 *lys*Y (Fig. S1) which are capable of forming
382 disulfide bonds (Lobstein *et al.*, 2012). We obtained a yield of 0.1mg of pure protein per
383 litre of culture. After peptide purification, UPLC-ESI-HRMS analysis of the purified
384 AgLTP24 protein revealed a monoisotopic $[M+H]^+$ m/z 9686.8008 (theoretical
385 monoisotopic m/z calculated for $C_{415}H_{676}N_{123}O_{126}S_9$: 9686.7760) consistent with the
386 formation of four disulfide bridges (Fig. S4). This analysis was made after each run of
387 purification and before bioassays to check the purity and the good conformation of the
388 protein with disulphide bridges.
389
390 **Physiology of *Frankia alni* in contact with AgLTP24**
391 A miniaturised, rapid and fluorescent bioassay using resazurin dye was successfully
392 developed to determine whether AgLTP24 had antimicrobial activity against *Frankia*
393 *alni* at 7 dpi. For this, we applied a range of concentrations of AgLTP24 from 1 to 5µM
394 (Fig. 4) and used kanamycin as positive control of inhibition of *Frankia*. The cell viability
395 of *Frankia* is reduced from a concentration of 5µM AgLTP24 (54 ± 16% of cell viability)
396 while no effect was detected below this concentration. AgLTP24 can thus be considered
397 an antibacterial peptide against the symbiotic partner at this concentration. In addition,
398 microscopy observation showed a negative effect of AgLTP24 on vesicles' production
399 (Fig. **4b**). Indeed, at 5µM of AgLTP24, no vesicle was observed whereas they are present

400 at sub-inhibitory concentrations. However, *Frankia* must be viable and efficient in the
401 nodule to ensure nitrogen fixation for trophic exchange with its plant partner. This
402 conducted us to perform a second physiological assay by using sub-inhibitory
403 concentrations of AgLTP24. The second physiological assay was conducted with a range
404 of AgLTP24 from 1nM to 1µM (Fig. 5). In this test, nitrogen fixation, respiratory activity
405 (OD_{490nm}) and growth effects (OD_{600nm}) were monitored over a 10 days' time course (Fig.
406 S5).
407 That range of AgLTP24 had little effect on *Frankia* growth. We noted a negative effect at
408 10nM of AgLTP24 on respiratory activity at early time of the time course (Fig. **S5b**) but
409 it was not maintained over time. Regarding respiratory activity, we observed a positive
410 but not significant effect with AgLTP24 above 100nM and 5 days of growth. The most
411 striking effect was observed on nitrogen fixation after 7 days of culture (Fig. 5) with a
412 concentration above 100nM leading to inhibitory effect whereas no effect was observed
413 on growth or respiratory activity. Conversely, at 1nM of this peptide, the AgLTP24
414 improved this activity. Microscopy did show any effect on vesicle morphology (data not
415 shown).
416

417 **Discussion**

418 Early steps of the interaction between alder and *Frankia* start with the molecular
419 dialogue through the secretion of flavonoids by the plant (Benoit & Berry, 1997; Hughes
420 *et al.*, 1999) and the bacterial "Nod-like" factors by *Frankia* (Cérémonie *et al.*, 1999;
421 Perrine-Walker *et al.*, 2011). This factor also called root hair deforming factor (RHDF)
422 because it triggers plant response by reorientating root-hair tip growth followed by the
423 formation of an infection thread (IT) and cell division induction in inner cortical cells.
424 This process leads to a nodule where *Frankia* will be housed and exchange with its plant

425 partner. Even though RHDF structure remains unknown, previous studies have shown
426 that this factor of around 3KDa is present in *Frankia* cell free supernatant and acts at
427 nanomolar dose (Cissoko *et al.*, 2018). In addition, this factor is able to induce a high
428 frequency nuclear Ca^{2+} spiking (Granqvist *et al.*, 2015). Due to the lack of a genetic
429 transformation system for alder, other approaches besides genetic inactivation have
430 been used to identify the host symbiotic determinants.
431 Focusing at nodule step (Hocher, V. *et al.*, 2011), transcriptomic analysis showed that
432 the common symbiotic cascade known in Legumes (interacting with rhizobia) and in
433 most land plants (interacting with VAM fungi) (Genre & Russo, 2016) was also present
434 in actinorhizal plants (Gherbi *et al.*, 2008; Hocher, V. *et al.*, 2011; Hocher, Valérie *et al.*,
435 2011). Previously, differential screening of cDNA libraries from root and nodules of
436 *Alnus glutinosa* with nodule and root cDNAs permitted to identify several symbiotic
437 genes among which a subtilisin-like protease (Ribeiro *et al.*, 1995), a sucrose synthase,
438 an enolase (van Ghelue *et al.*, 1996), and a dicarboxylate transporter (Jeong *et al.*, 2004).
439 These genes are evocative of tissue reorganization and trophic exchanges but shed no
440 light on the triggering of organogenesis. The present study aimed at investigating the
441 plant molecular response at early symbiotic stages by using same transcriptomic
442 microarray as in our previous work at nodule step (Hocher, V. *et al.*, 2011).
443

444 **Global plant response at early step of symbiosis**

445 Firstly, the two experiments induced different level of response in the plant partners
446 with stronger signal in the Exp1, suggesting that even though the supernatant is
447 sufficient to trigger root-hair deformation, a sustained dynamic of interaction with
448 *Frankia* is more efficient. These results suggest that *Frankia* secretome produced during
449 Exp1 could be more diverse triggering a strong perception of its presence by plant.

450 Indeed, *Frankia* secretes a variety of proteolytic enzymes such as glycosidases,
451 esterases, or proteases presumably involved in root infection (Mastronunzio *et al.*,
452 2008).
453 Plant global response reveals a common pattern with a strong modulation of genes
454 involved in stress response. This biological process, specific to early response (Hocher,
455 V. *et al.*, 2011) is constituted by genes encoding putative proteins involved in oxidative
456 stress (oxidase, peroxidase); to defense against pathogens such as pathogenesis related
457 (PR) proteins (chitinase, Defensin, thaumatin or nsLTP). Beside these biological
458 processes, we can propose different steps in the plant response after *Frankia* contact.
459
460 *Oxidative stress in hairy roots repressed in nodule*
461 Focusing on oxidative stress, both the overall GO analysis showed a strong induction of
462 genes involved in oxido-reduction metabolism (oxidase, peroxidase). These enzymes
463 involved in oxidative stress to reduce reactive oxygen species (ROS) suggesting that
464 *Frankia* supernatant induces a ROS stress such as previously observed for rhizobia at
465 early steps of interaction (Peleg-Grossman *et al.*, 2009; Peleg-Grossman *et al.*, 2012). In
466 legume roots, the enzymatic activities of catalase, ascorbate peroxidase, glutathione
467 reductase or NADPH oxidase significantly increase upon inoculation with bacterial
468 symbiont (Bueno *et al.*, 2001; Den Herder *et al.*, 2007; Peleg-Grossman *et al.*, 2009;
469 Peleg-Grossman *et al.*, 2012). After this important release, ROS production reduced
470 drastically to prevent root hair curling and IT formation (Shaw & Long, 2003; Lohar *et*
471 *al.*, 2007).
472 To follow this dynamics of expression over the course of symbiosis establishment, we
473 extracted transcriptional data from our previous work made at nodule step (Hocher, V.
474 *et al.*, 2011). Few genes are not modulated or repressed in the nodule steps (Table S4,

475 Fig. **2**), suggesting a similar profile. Consequently, plant after *Frankia* internalization
476 would repress this stress response but the measure of ROS abundance over the time
477 course of the symbiosis is necessary to support this tendency.
478
479 *Perception of Frankia factor, signaling and hormonal function*
480 Little is known about the symbiotic signals produced by *Frankia* but their perception
481 requires plant receptor. Here, a statistical analysis revealed a moderate
482 overrepresentation of gene involved in signal transduction (Table 1; AG-N01f_037_C05)
483 encoding a putative receptor like kinase (RLK) somewhat repressed in the nodule
484 suggesting its potential implication in *Frankia* recognition. However, other RLK similar
485 to Lys6/Lys7/Nfr1 of legume NF receptors (AG-R01f_025_F02) already found in *A.*
486 *glutinosa* (Hocher, V. *et al.*, 2011) are not modulated after 2.5 days, which raises the
487 question of *Frankia* recognition. Plant RLKs have been shown to control the initiation,
488 development, and maintenance of symbioses with beneficial mycorrhizal fungi and
489 rhizobia (Buendia *et al.*, 2018; Chiu & Paszkowski, 2020) but the mechanism in
490 actinorhizal symbiosis remain unknown (Svistoonoff *et al.*, 2014).
491 The CSSP transduction will trigger primordium organogenesis where hormonal balance
492 plays a crucial function and particularly auxin. Indeed, exogenous auxins treatments
493 lead to the formation of thick lateral roots resembling nodules in actinorhizal Fagales
494 (Hammad *et al.*, 2003; Svistoonoff *et al.*, 2003) and an auxin influx inhibitor perturbs the
495 formation of nodules in another actinorhizal model, *Casuarina glauca* (Peret *et al.*,
496 2008). Transcriptional data at early steps sustain the pivotal function of auxin by
497 demonstrating the overexpression of several genes encoding auxin binding proteins
498 (Table 1: AGCL1169Contig1) or auxin inducing proteins (Table S2: AGCL1376Contig1;
499 AG-N01f_043_C20). We did not detected genes involved in salicylic acid (SA) or jasmonic

500 acid (JA) biosynthesis in early steps of symbiosis however a fine bioinformatics study of
501 metabolic routes using the genome alder is required to facilitate putative assignation
502 and to validate or not their absence in those omic data.
503 In any case, perception of pathogen by plant triggers SA and JA accumulation and leads
504 to the accumulation of PR proteins to minimize pathogen load or disease onset. In
505 legume symbiosis, those hormones inhibit bacterial infection and nodule development
506 (Liu *et al.*, 2018) suggesting that NF recognition represses this accumulation.
507
508 *Defense mechanisms activation*
509 After oxidative stress, following *Frankia* contact, alder activates numerous genes
510 encoding PR proteins which are key components of plant innate immune system against
511 both biotic and abiotic stresses (Ali *et al.*, 2018). More precisely, PR proteins have
512 diverse functions such as glucanase, chitinases, thaumatin like, peroxidases, defensins,
513 nsLTPs or thionins.
514 We found numerous upregulated chitinases as observed in legumes (Staehelin *et al.*,
515 1994; Goormachtig *et al.*, 1998; Xie *et al.*, 1999) and described as important for rhizobia
516 infection and IT formation (Malolepszy *et al.*, 2018). Also, genes for oxidative stress and
517 chitinases are not modulated or repressed in late step of actinorhizal symbiosis (Table
518 S4, Fig. **2**) suggesting they are important in the early steps of *Frankia* infection.
519 Furthermore, genes encoding one uncharacterized PR proteins is upregulated after
520 *Frankia* contact (AG-R01f_016_N10) and rapidly repressed at nodule step (Table 1). A
521 similar profile was observed for PR10 in *Medicago trunculata* when associated to
522 symbiont or pathogen infection, it is activated but in symbiotic pathway, its expression
523 is transitory suggesting that defense signaling pathways are suppressed during the
524 establishment of symbiosis (Chen *et al.*, 2017). Here, the transitory activation of the

525 Alder PR protein could be also induced by *Frankia* factors even though a specific
526 response must be demonstrated by comparing to other biotic and abiotic stresses.
527 Some of the PR proteins are classified as AMPs based on their small size, the
528 conservation of cysteine rich motif and their potential action as antimicrobial compound
529 (Tam *et al.*, 2015). In alder transcriptome, we distinguished the overexpression of gene
530 encoding plant defensins (Ag3, Ag5 and Ag11), thaumatins (AG-N01f_038_P13) and
531 nsLTPs (AGCL115Contig1). Here, all AMPs induced at early steps are still overexpressed
532 in nodule (Table S4, Fig. **2**).
533 Like defensin, thaumatin like proteins considered as a member of defense protein but
534 also in plant development (de Jesús-Pires *et al.*, 2020) is overinduced in alder during
535 actinorhizal symbiosis. This expression profile is quite different to the well-documented
536 thaumatin like gene in soybean. Indeed, the *rj4* thaumatin like gene was described as
537 constitutively and similarly transcribed in roots and nodules and intervene at a very
538 early stage of IT formation to inhibit nodule formation with an incompatible strain
539 (Hayashi *et al.*, 2014). This suggests that thaumatin-like proteins in alder could
540 intervene in incompatibility function but its overexpression in nodule step also raise
541 question about another function in nodule organogenesis.
542
543 **AgLTP24: from *Frankia* infection to nodule functioning**
544 *Function at early step*
545 Global omic approach made at early steps of alder symbiosis pointed to a strong signal
546 from one protein belonging to nsLTPs family named here AgLTP24. The
547 immunolocalization on curled hairy roots induced after *Frankia* contact showed the
548 specific binding of AgLTP24 in nooks (Fig. **3**) where *Frankia* embedding before
549 internalization through IT formation. This suggests that AgLTP24 acts at the early phase

550 of infection. This is supported the induction of an nsLTP (MtN5) in *M. trunculata* at early
551 stage of symbiosis and in the nodule (Pii *et al.*, 2009; Pii *et al.*, 2012). Because its
552 silencing resulted in an increased number of curling events with a reduced number of
553 invading primordia, whereas its overexpression resulted in an increased number of
554 nodules, authors concluded that MtN5 is important at very early step of infection for the
555 successful establishment of the symbiotic interaction but not in nodule formation (Pii *et*
556 *al.*, 2013). Similar to MtN5 (Pii *et al.*, 2009), AgLTP24 possesses a slight antimicrobial
557 activity *in vitro* against its symbiont at 5µM. As *Frankia* cell integrity must be preserved
558 for infection, we hypothesize that AgLTP24 concentration in contact with *Frankia* must
559 be below to 5µM. Further investigation to assess protein concentration in plant tissues is
560 a great challenge but requires the development of high-performance mass spectrometry
561 technology coupled to imagery (Gemperline *et al.*, 2015; Gemperline *et al.*, 2016).
562 Finally, AgLTP24 could be a gene player at early step of symbiosis to transduce signal
563 within plant roots to permit IT formation as well as induce stress response in *Frankia*
564 cells.
565
566 *Function at late step*
567 *AgLTP24* is also present in nodule (Table 1) and targets specifically *Frankia's* vesicle in
568 nodule fixation zone (Fig. **3f**) but this localization is different from MtN5 binding in the
569 distal zone of the nodule (Pii *et al.*, 2012). However, a nsLTP (AsE246) found in
570 *Astragalus sinicus* specifically symbiosome membranes through binding a lipid
571 component: digalactosyldiacylglycerol (DGG) (Lei *et al.*, 2014). In this model, the *asE246*
572 silencing impacts nodule development with fewer matured infected plant cells.
573 Thus, AgLTP24 could fix vesicle wall composed by a multilamellate hopanoid lipid
574 envelopes (Berry *et al.*, 1993; Nalin *et al.*, 2000) or plant perisymbiontic membrane

575 coating *Frankia* cells in nodule. The perisymbiosome membrane composition is less
576 documented but non-inoculated *Alnus rubra* roots are mainly composed of glycerol,
577 phosphatidylethanolamine, phosphatidylserine and phosphatidylcholine (Berry *et al.*,
578 1991). A lipidomic study in *A. glutinosa* roots using recent technology followed by a
579 bioassay binding is a great perspective to decipher AgLTP24 mechanisms involved.
580 As observed *in vitro*, AgLTP24 could act as antimicrobial compound by reducing cell
581 viability and vesicles formation of *Frankia* (Fig. 4) suggesting a potential role by
582 controlling *Frankia* proliferation in nodule. However, because expression of nitrogen
583 fixation gene cluster is more active in symbiotic conditions compared to N-free culture
584 condition (Alloisio *et al.*, 2010; Lurthy *et al.*, 2018), the concentration probably present
585 in the nodule fixation zone would be lower to this lethal concentration. It is worth to
586 note that at 1nM concentration of AgLTP24, the nitrogen fixation activity is induced a
587 higher but not statistically so significant without perturbing *Frankia* growth (Fig. 5). The
588 improvement of nitrogen fixation was also observed for the AgDef5 defensin
589 translocated by *A. glutinosa* to *Frankia*'s vesicle in nodule (Carro *et al.*, 2015b).
590 In addition, this defensin is also upregulated at 2.5 dpi (Table 1) suggesting the plant
591 could deliver a cocktail of molecules including AgLTP24 to improve bacterial infection
592 and nitrogen fixation in nodule. A depth investigation of this synergic effect *in vitro*
593 opens a new perspective in addition to their genetic silencing in plant as an exciting
594 challenge to complete the gap of knowledge regarding their role in actinorhizal
595 symbiosis.
596

597 **Acknowledgements**

598 Thanks are expressed to Elise Lacroix and the Greenhouse facility (FR 41), to Danis
599 Abrouk in the ibio platform for help in submission of omic data to international

database, Jonathan Gervaix in the AME platform to access ARA measurement and Philippe Bulet for his technical advice on peptide purification. We thank the PGE platform for other measurements. This project has been funded by the FR BioEnviS (Biodiversité, Environnement et Santé, Université Lyon1, France) and the EC2CO (Ecosphère Continentale et Côtière) grant (reference: 10459).

Author contribution

M.G., N.A., A.H., P.N., P.P. and H.B. conceived and designed the study. M.G., N.A., P.F., S.B., O.K, J.T., P.D.S., P.P and H.B carried out the experiments. M.G., P.N., P.P. and H.B. performed the data analysis. M.G., P.D.S., and H.B. performed the figure drawing. M.G., P.N., P.P., A.H. and H.B. provided critical biological interpretations of the data. P.N. and H.B. wrote the manuscript.

Competing Interests

The authors declare no competing interests.

Bibliography

Ali S, Ganai BA, Kamili AN, Bhat AA, Mir ZA, Bhat JA, Tyagi A, Islam ST, Mushtaq M, Yadav P, et al. 2018. Pathogenesis-related proteins and peptides as promising tools for engineering plants with multiple stress tolerance. *Microbiological Research* **212-213**: 29-37.

Alloisio N, Queiroux C, Fournier P, Pujic P, Normand P, Vallenet D, Medigue C, Yamaura M, Kakoi K, Kucho K. 2010. The *Frankia alni* symbiotic transcriptome. *Mol Plant Microbe Interact* **23**(5): 593-607.

Benoit LF, Berry AM. 1997. Flavonoid-like compounds from seeds of red alder (Alnus rubra) influence host nodulation by Frankia (Actinomycetales). *Physiologia Plantarum* **99**(4): 588-593.

Berry AM, Harriott OT, Moreau RA, Osman SF, Benson DR, Jones AD. 1993. Hopanoid lipids compose the *Frankia* vesicle envelope, presumptive barrier of

629 oxygen diffusion to nitrogenase. *Proceedings of the National Academy of Sciences*
630 **90**(13): 6091-6094.

631 **Berry AM, Moreau RA, Jones AD. 1991.** Bacteriohopanetetrol: abundant lipid in
632 frankia cells and in nitrogen-fixing nodule tissue. *Plant Physiol* **95**(1): 111-115.

633 **Berry AM, Torrey JG. 1983.** Root hair deformation in the infection process of Alnus
634 rubra. *Botany* **61**: 2863-2876.

635 **Brooks JM, Benson DRJS. 2016.** Comparative metabolomics of root nodules infected
636 with Frankia sp. strains and uninfected roots from Alnus glutinosa and Casuarina
637 cunninghamiana reflects physiological integration. *Symbiosis* **70**(1): 87-96.

638 **Buendia L, Girardin A, Wang T, Cottret L, Lefebvre B. 2018.** LysM Receptor-Like
639 Kinase and LysM Receptor-Like Protein Families: An Update on Phylogeny and
640 Functional Characterization. *Frontiers in Plant Science* **9**(1531).

641 **Bueno P, Soto MJ, Rodríguez-Rosales MP, Sanjuan J, Olivares J, Donaire JP. 2001.**
642 Time-course of lipoxygenase, antioxidant enzyme activities and H2O2
643 accumulation during the early stages of Rhizobium–legume symbiosis. *New*
644 *Phytologist* **152**(1): 91-96.

645 **Carro L, Persson T, Pujic P, Alloisio N, Fournier P, Boubakri H, Pawlowski K,**
646 **Normand P. 2015a.** Organic acids metabolism in *Frankia alni*. *Symbiosis* **70**(1):
647 37-48.

648 **Carro L, Pujic P, Alloisio N, Fournier P, Boubakri H, Hay AE, Poly F, Francois P,**
649 **Hocher V, Mergaert P, et al. 2015b.** *Alnus* peptides modify membrane porosity
650 and induce the release of nitrogen-rich metabolites from nitrogen-fixing *Frankia*.
651 *ISME J* **9**(8): 1723-1733.

652 **Carro L, Pujic P, Alloisio N, Fournier P, Boubakri H, Poly F, Rey M, Heddi A,**
653 **Normand P. 2016.** Physiological effects of major up-regulated Alnus glutinosa
654 peptides on Frankia sp. ACN14a. *Microbiology* **162**(7): 1173-1184.

655 **Cérémonie H, Debellé F, Fernandez MP. 1999.** Structural and functional comparison
656 of Frankia root hair deforming factor and rhizobia Nod factor. *Canadian Journal of*
657 *Botany* **77**(9): 1293-1301.

658 **Chen T, Duan L, Zhou B, Yu H, Zhu H, Cao Y, Zhang Z. 2017.** Interplay of Pathogen-
659 Induced Defense Responses and Symbiotic Establishment in Medicago truncatula.
660 *Frontiers in Microbiology* **8**: 973-973.

661 **Chiu CH, Paszkowski U. 2020.** Receptor-Like Kinases Sustain Symbiotic
662 Scrutiny1 [OPEN]. *Plant Physiology* **182**(4): 1597-1612.

663 **Chung CT, Niemela SL, Miller RH. 1989.** One-step preparation of competent
664 Escherichia coli: transformation and storage of bacterial cells in the same
665 solution. *Proc Natl Acad Sci U S A* **86**(7): 2172-2175.

666 **Cissoko M, Hocher V, Gherbi H, Gully D, Carré-Mlouka A, Sane S, Pignoly S,**
667 **Champion A, Ngom M, Pujic P, et al. 2018.** Actinorhizal Signaling Molecules:
668 *Frankia* Root Hair Deforming Factor Shares Properties With NIN Inducing Factor.
669 *Frontiers in Plant Science* **9**(1494).

670 **Conesa A, Gotz S. 2008.** Blast2GO: A comprehensive suite for functional analysis in
671 plant genomics. *Int J Plant Genomics* **2008**: 619832.

672 **D'Haeze W, Holsters M. 2002.** Nod factor structures, responses, and perception during
673 initiation of nodule development. *Glycobiology* **12**(6): 79R-105R.

674 **de Jesús-Pires C, Ferreira-Neto JRC, Pacifico Bezerra-Neto J, Kido EA, de Oliveira**
675 **Silva RL, Pandolfi V, Wanderley-Nogueira AC, Binneck E, da Costa AF, Pio-**
676 **Ribeiro G, et al. 2020.** Plant Thaumatin-like Proteins: Function, Evolution and
677 Biotechnological Applications. *Curr Protein Pept Sci* **21**(1): 36-51.

678 **Den Herder J, Lievens S, Rombauts S, Holsters M, Goormachtig S. 2007.** A Symbiotic
679 Plant Peroxidase Involved in Bacterial Invasion of the Tropical Legume Sesbania
680 rostrata *Plant Physiology* **144**(2): 717-727.

681 **Edstam MM, Viitanen L, Salminen TA, Edqvist J. 2011.** Evolutionary history of the
682 non-specific lipid transfer proteins. *Mol Plant* **4**(6): 947-964.

683 **Fahraeus G. 1957.** The infection of clover root hairs by nodule bacteria studied by a
684 simple glass slide technique. *J Gen Microbiol* **16**(2): 374-381.

685 **Fu C, Donovan WP, Shikapwashya-Hasser O, Ye X, Cole RH. 2014.** Hot Fusion: an
686 efficient method to clone multiple DNA fragments as well as inverted repeats
687 without ligase. *PLoS One* **9**(12): e115318.

688 **Gemperline E, Jayaraman D, Maeda J, Ane JM, Li L. 2015.** Multifaceted investigation
689 of metabolites during nitrogen fixation in Medicago via high resolution MALDI-
690 MS imaging and ESI-MS. *J Am Soc Mass Spectrom* **26**(1): 149-158.

691 **Gemperline E, Keller C, Jayaraman D, Maeda J, Sussman MR, Ané JM, Li L. 2016.**
692 Examination of Endogenous Peptides in Medicago truncatula Using Mass
693 Spectrometry Imaging. *J Proteome Res* **15**(12): 4403-4411.

694 **Genre A, Russo G. 2016.** Does a common pathway transduce symbiotic signals in plant–
695 microbe interactions? *Front Plant Sci.* **7**: 96.

696 **Ghelue MV, Løvaas E, Ringø E, Solheim B. 1997.** Early interactions between Alnus
697 glutinosa and Frankia strain ArI3. Production and specificity of root hair
698 deformation factor(s). *Physiologia Plantarum* **99**(4): 579-587.

699 **Gherbi H, Markmann K, Svistoonoff S, Estevan J, Autran D, Giczey G, Auguy F, Peret**
700 **B, Laplaze L, Franche C, et al. 2008.** SymRK defines a common genetic basis for
701 plant root endosymbioses with arbuscular mycorrhiza fungi, rhizobia, and
702 Frankiabacteria. *Proc Natl Acad Sci U S A* **105**(12): 4928-4932.

703 **Goormachtig S, Lievens S, Van de Velde W, Van Montagu M, Holsters M. 1998.**
704 Srchi13, a Novel Early Nodulin from Sesbania rostrata, Is Related to Acidic Class
705 III Chitinases. *The Plant Cell* **10**(6): 905-915.

706 **Granqvist E, Sun J, Op den Camp R, Pujic P, Hill L, Normand P, Morris RJ, Downie JA,**
707 **Geurts R, Oldroyd GE. 2015.** Bacterial-induced calcium oscillations are common
708 to nitrogen-fixing associations of nodulating legumes and nonlegumes. *New*
709 *Phytol* **207**(3): 551-558.

710 **Griesmann M, Chang Y, Liu X, Song Y, Haberer G, Crook MB, Billault-Penneteau B,**
711 **Lauressergues D, Keller J, Imanishi L, et al. 2018.** Phylogenomics reveals
712 multiple losses of nitrogen-fixing root nodule symbiosis. *Science* **361**(6398):
713 eaat1743.

714 **Hammad Y, Nalin R, Marechal J, Fiasson K, Pepin Rg, Berry AM, Normand P,**
715 **Domenach A-M. 2003.** A possible role for phenyl acetic acid (PAA) on Alnus
716 glutinosa nodulation by Frankia. *Plant Soil* **254**(1): 193-205.

717 **Hay A-E, Herrera-Belaroussi A, Rey M, Fournier P, Normand P, Boubakri H. 2020.**
718 Feedback Regulation of N Fixation in Frankia-Alnus Symbiosis Through Amino
719 Acids Profiling in Field and Greenhouse Nodules. *Molecular Plant-Microbe*
720 *Interactions®* **33**(3): 499-508.

721 **Hay AE, Boubakri H, Buonomo A, Rey M, Meiffren G, Cotin-Galvan L, Comte G,**
722 **Herrera-Belaroussi A. 2017.** Control of endophytic *Frankia* sporulation by
723 Alnus nodule metabolites. *Mol Plant Microbe Interact* **30**: 205-214.

724 **Hayashi M, Shiro S, Kanamori H, Mori-Hosokawa S, Sasaki-Yamagata H, Sayama T,**
725 **Nishioka M, Takahashi M, Ishimoto M, Katayose Y, et al. 2014.** A Thaumatin-
726 Like Protein, Rj4, Controls Nodule Symbiotic Specificity in Soybean. *Plant and Cell*
727 *Physiology* **55**(9): 1679-1689.

728 **Hocher V, Alloisio N, Auguy F, Fournier P, Doumas P, Pujic P, Gherbi H, Queiroux C,**
729 **Da Silva C, Wincker P, et al. 2011.** Transcriptomics of actinorhizal symbioses
730 reveals homologs of the whole common symbiotic signaling cascade. *Plant*
731 *Physiol* **156**(2): 700-711.

732 **Hocher V, Alloisio N, Bogusz D, Normand P. 2011.** Early signaling in actinorhizal
733 symbioses. *Plant signaling & behavior* **6**(9): 1377-1379.

734 **Hughes M, Donnelly C, Crozier A, Wheeler CT. 1999.** Effects of the exposure of roots
735 of Alnus glutinosa to light on flavonoids and nodulation. *Canadian Journal of*
736 *Botany* **77**(9): 1311-1315.

737 **Jeong J, Suh S, Guan C, Tsay YF, Moran N, Oh CJ, An CS, Demchenko KN, Pawlowski**
738 **K, Lee Y. 2004.** A nodule-specific dicarboxylate transporter from alder is a
739 member of the peptide transporter family. *Plant Physiol* **134**(3): 969-978.

740 **Ktari A, Gueddou A, Nouioui I, Miotello G, Sarkar I, Ghodhbane-Gtari F, Sen A,**
741 **Armengaud J, Gtari M. 2017.** Host Plant Compatibility Shapes the
742 Proteogenome of *Frankia coriariae*. *Front Microbiol* **8**: 720.

743 **Lalonde M. 1979.** Immunological and Ultrastructural Demonstration of Nodulation of
744 the European Alnus glutinosa (L.) Gaertn. Host Plant by an Actinomycetal Isolate
745 from the North American Comptonia peregrina (L.) Coult. Root Nodule. *Botanical*
746 *Gazette* **140**: S35-S43.

747 **Lei L, Chen L, Shi X, Li Y, Wang J, Chen D, Xie F, Li Y. 2014.** A Nodule-Specific Lipid
748 Transfer Protein AsE246 Participates in Transport of Plant-Synthesized Lipids to
749 Symbiosome Membrane and Is Essential for Nodule Organogenesis in Chinese
750 Milk Vetch. *Plant Physiology* **164**(2): 1045-1058.

751 **Liu H, Zhang C, Yang J, Yu N, Wang E. 2018.** Hormone modulation of legume-rhizobial
752 symbiosis. *Journal of Integrative Plant Biology* **60**(8): 632-648.

753 **Lobstein J, Emrich CA, Jeans C, Faulkner M, Riggs P, Berkmen M. 2012.** SHuffle, a
754 novel Escherichia coli protein expression strain capable of correctly folding
755 disulfide bonded proteins in its cytoplasm. *Microbial cell factories* **11**: 56-56.

756 **Login FH, Balmand S, Vallier A, Vincent-Monégat C, Vigneron A, Weiss-Gayet M,**
757 **Rochat D, Heddi A. 2011.** Antimicrobial peptides keep insect endosymbionts
758 under control. *Science* **334**(6054): 362-365.

759 **Lohar DP, Haridas S, Gantt JS, VandenBosch KA. 2007.** A transient decrease in
760 reactive oxygen species in roots leads to root hair deformation in the legume-
761 rhizobia symbiosis. *New Phytol* **173**(1): 39-49.

762 **Lurthy T, Alloisio N, Fournier P, Anchisi S, Normand P, Pujic P, Boubakri H. 2018.**
763 Molecular response to nitrogen starvation by *Frankia alni* ACN14a revealed by
764 transcriptomics and functional analysis with a fosmid library in Escherichia coli.
765 *Research in Microbiology*

766 **Malolepszy A, Kelly S, Sørensen KK, James EK, Kalisch C, Bozsoki Z, Panting M,**
767 **Andersen SU, Sato S, Tao K, et al. 2018.** A plant chitinase controls cortical
768 infection thread progression and nitrogen-fixing symbiosis. *eLife* **7**: e38874.

769 **Mastronunzio JE, Tisa LS, Normand P, Benson DR. 2008.** Comparative secretome
770 analysis suggests low plant cell wall degrading capacity in *Frankia* symbionts.
771 *BMC Genomics* **9**: 47.

772 **Nalin R, Putra S, Domenach AM, Rohmer M, Gourbière F, Berry A. 2000.** High
773 hopanoid/total lipids ratio in Frankia mycelia is not related to the nitrogen
774 status. *Microbiology* **146 (Pt 11)**: 3013-3019.

775 **Navarro E, Bousquet J, Moiroud A, Munive A, Piou D, Normand P. 2003.** Molecular
776 phylogeny of Alnus (Betulaceae), inferred from nuclear ribosomal DNA ITS
777 sequences. *Plant and Soil* **254**(1): 207-217.

778 **Normand P, Fernandez MP 2019.** *Frankia. Bergey's Manual of Systematics of Archaea*
779 *and Bacteria*: (eds W.B. Whitman, F.A. Rainey, P. Kämpfer, M.E. Trujillo, P. DeVos,
780 B. Hedlund and S. Dedysh), 1-19.

781 **Normand P, Lalonde M. 1982.** Evaluation of *Frankia* strains isolated from provenances
782 of two Alnus species. *Canadian Journal of Microbiology* **28**(10): 1133-1142.

783 **Normand P, Lapierre P, Tisa LS, Gogarten JP, Alloisio N, Bagnarol E, Bassi CA, Berry**
784 **AM, Bickhart DM, Choisne N, et al. 2007.** Genome characteristics of
785 facultatively symbiotic *Frankia* sp. strains reflect host range and host plant
786 biogeography. *Genome Res* **17**(1): 7-15.

787 **Peleg-Grossman S, Golani Y, Kaye Y, Melamed-Book N, Levine A. 2009.** NPR1
788 protein regulates pathogenic and symbiotic interactions between Rhizobium and
789 legumes and non-legumes. *PLoS One* **4**(12): e8399.

790 **Peleg-Grossman S, Melamed-Book N, Levine A. 2012.** ROS production during
791 symbiotic infection suppresses pathogenesis-related gene expression. *Plant*
792 *signaling & behavior* **7**(3): 409-415.

793 **Peret B, Svistoonoff S, Lahouze B, Auguy F, Santi C, Doumas P, Laplaze L. 2008.** A
794 Role for auxin during actinorhizal symbioses formation? *Plant Signal Behav* **3**(1):
795 34-35.

796 **Perrine-Walker F, Gherbi H, Imanishi L, Hocher V, Ghodhbane-Gtari F, Lavenus J,**
797 **Benabdoun FM, Nambiar-Veeti M, Svistoonoff S, Laplaze L. 2011.** Symbiotic
798 signaling in actinorhizal symbioses. *Curr Protein Pept Sci* **12**(2): 156-164.

799 **Pii Y, Astegno A, Peroni E, Zaccardelli M, Pandolfini T, Crimi M. 2009.** The Medicago
800 truncatula N5 gene encoding a root-specific lipid transfer protein is required for
801 the symbiotic interaction with Sinorhizobium meliloti. *Mol Plant Microbe Interact*
802 **22**(12): 1577-1587.

803 **Pii Y, Molesini B, Masiero S, Pandolfini T. 2012.** The non-specific lipid transfer
804 protein N5 of *Medicago truncatula* is implicated in epidermal stages of *rhizobium*-
805 host interaction. *BMC Plant Biol* **12**: 233.

806 **Pii Y, Molesini B, Pandolfini T. 2013.** The involvement of Medicago truncatula non-
807 specific lipid transfer protein N5 in the control of rhizobial infection. *Plant*
808 *signaling & behavior* **8**(7): e24836-e24836.

809 **Prin Y, Neyra M, Diem HG. 1990.** Estimation of *Frankia* growth using Bradford protein
810 and INT reduction activity estimations: application to inoculum standardization.
811 *FEMS Microbiology Letters* **69**(1-2): 91-95.

812 **Pujic P, Alloisio N, Fournier P, Roche D, Sghaier H, Miotello G, Armengaud J, Berry**
813 **AM, Normand P. 2019.** Omics of the early molecular dialogue between *Frankia*
814 *alni* and *Alnus glutinosa* and the cellulase synton. *Environmental Microbiology*
815 **0**(0).

816 **Ribeiro A, Akkermans AD, van Kammen A, Bisseling T, Pawlowski K. 1995.** A
817 nodule-specific gene encoding a subtilisin-like protease is expressed in early
818 stages of actinorhizal nodule development. *Plant Cell* **7**(6): 785-794.

819 **Schagger H. 2006.** Tricine-SDS-PAGE. *Nat Protoc* **1**(1): 16-22.

820 **Shaw SL, Long SR. 2003.** Nod factor inhibition of reactive oxygen efflux in a host
821 legume. *Plant Physiology* **132**(4): 2196-2204.

822 **Staehelin C, Granado J, Müller J, Wiemken A, Mellor RB, Felix G, Regenass M,**
823 **Broughton WJ, Boller T. 1994.** Perception of Rhizobium nodulation factors by
824 tomato cells and inactivation by root chitinases. *Proceedings of the National*
825 *Academy of Sciences* **91**(6): 2196-2200.

826 **Svistoonoff S, Hocher V, Gherbi H. 2014.** Actinorhizal root nodule symbioses: what is
827 signalling telling on the origins of nodulation? *Curr Opin Plant Biol* **20C**: 11-18.

828 **Svistoonoff S, Laplaze L, Auguy F, Runions J, Duponnois R, Haseloff J, Franche C,**
829 **Bogusz D. 2003.** cg12 expression is specifically linked to infection of root hairs
830 and cortical cells during *Casuarina glauca* and *Allocasuarina verticillata*
831 actinorhizal nodule development. *Mol Plant Microbe Interact* **16**(7): 600-607.

832 **Tam JP, Wang S, Wong KH, Tan WL. 2015.** Antimicrobial Peptides from Plants.
833 *Pharmaceuticals* **8**(4): 711-757.

834 **van Ghelue M, Ribeiro A, Solheim B, Akkermans AD, Bisseling T, Pawlowski K.**
835 **1996.** Sucrose synthase and enolase expression in actinorhizal nodules of Alnus
836 glutinosa: comparison with legume nodules. *Mol Gen Genet* **250**(4): 437-446.

837 **Xie Z-P, Staehelin C, Wiemken A, Broughton WJ, Müller J, Boller T. 1999.** Symbiosis-
838 stimulated chitinase isoenzymes of soybean (Glycine max (L.) Merr.). *Journal of*
839 *Experimental Botany* **50**(332): 327-333.
840

841 **Figure legends**

842

843 **Table 1:** The up-regulated genes during early root hair deformation of *Alnus glutinosa* in
844 both experiments, with *Frankia* indirect contact (FIndC) and with *Frankia* supernatant
845 contact (FSupC).

846

847 **Figure 1:** Gene Ontology (GO) functional classification analysis. A. Distribution of
848 annotated genes into functional categories according to GO biological process. B. GO
849 functional classification analysis was made by comparing (A) up and down-regulated
850 genes found in Exp1 (Table S2) according to biological process, molecular function and

851 cellular component through Fisher test. Number of sequences (Nr) were indicated for
852 each category. BLAST2GO pipeline was used to get this GO annotation.
853
854 **Figure 2:** Expression levels of the genes which were commonly upregulated and
855 downregulated in FindC and FsupC conditions. The expression level values in nodule
856 were extracted from our previous work ((5); Table S4). The expression values were
857 expressed as Fold change (FC) with a color gradient from red (down-regulated; ≤0.5)
858 and orange-yellow (no-regulated) to green (up-regulated; ≥2) in infected roots or
859 nodules compared to control roots without Frankia. The GO annotations were assigned
860 by noting preferentially biological process and if not present, the molecular function.
861 Certain genes have no GO assignation after blast2Go analysis. The heatmap was
862 generated by GraphPad Prism 9.2.0.
863
864 **Figure 3:** AgLTP24 localization in roots after 2.5 days (A, B,C) or nodule of 21 dpi (D, E,
865 F). Hair magnification of a specific zone of the infected root (C) or nodule (F).
866 Immunofluorescence localization of AgLTP24 in hairy roots (B, C) and around Frankia
867 vesicles in infected cells (E and F). Negative control with rabbit serum before
868 intramuscular injection of AgLTP24 epitope (A, D) showed no green fluorescence in
869 hairy roots (A) or infected cells (D).
870 Blue: DAPI; red: autofluorescence; green: Alexa Fluor 488 dye anti-rabbit antibody (Life
871 Technologies, Saint Aubin, France). c, infected cells; nc, noninfected cells; v, *Frankia*
872 vesicles; x, xylem.
873
874 **Figure 4: physiological bioassays on *Frankia* growth and cellular development**. **A.**
875 Resazurin bioassay on *Frankia* ACN14a growth after supplementation of 1 to 5µM of

876 AgLTP24. Cell viability was calculated by normalizing the fluorescence of the assay with
877 the mean of the negative control (*Frankia* without AgLTP24). Kanamycin (40µg.ml^{-1})
878 was used as positive control. Data are expressed as mean values ± SD. Differences
879 between normalized data were assessed by the Mann Whitney test (bilateral and
880 unpaired) compared to control. Graphic representation and statistical analysis of results
881 was conducted with GraphPad Prism version 9.2.0. *p value <0.05, **p value <0.01.
882 **B.** *Frankia* cells observation without or with gradual concentration of AgLTP24 from 0
883 (Control) to 5µM and obtained during the different physiological bioassays. v, *Frankia*
884 vesicles
885
886 **Figure 5: effect of AgLTP24 in physiology of *Frankia*** after 7 days of growth on **A.**
887 Nitrogen fixation; **B.** respiratory activity and **C.** growth by measuring OD_{600nm}. Data were
888 extracted from the kinetic assay (Fig. S5).
889 Data are expressed as mean values ± SD. Differences between means were assessed by
890 the Mann Whitney test (bilateral and unpaired) compared to control. Graphic
891 representation and statistical analysis of results was conducted with GraphPad Prism
892 9.2.0. *p value <0.05, **p value < 0.01.
893

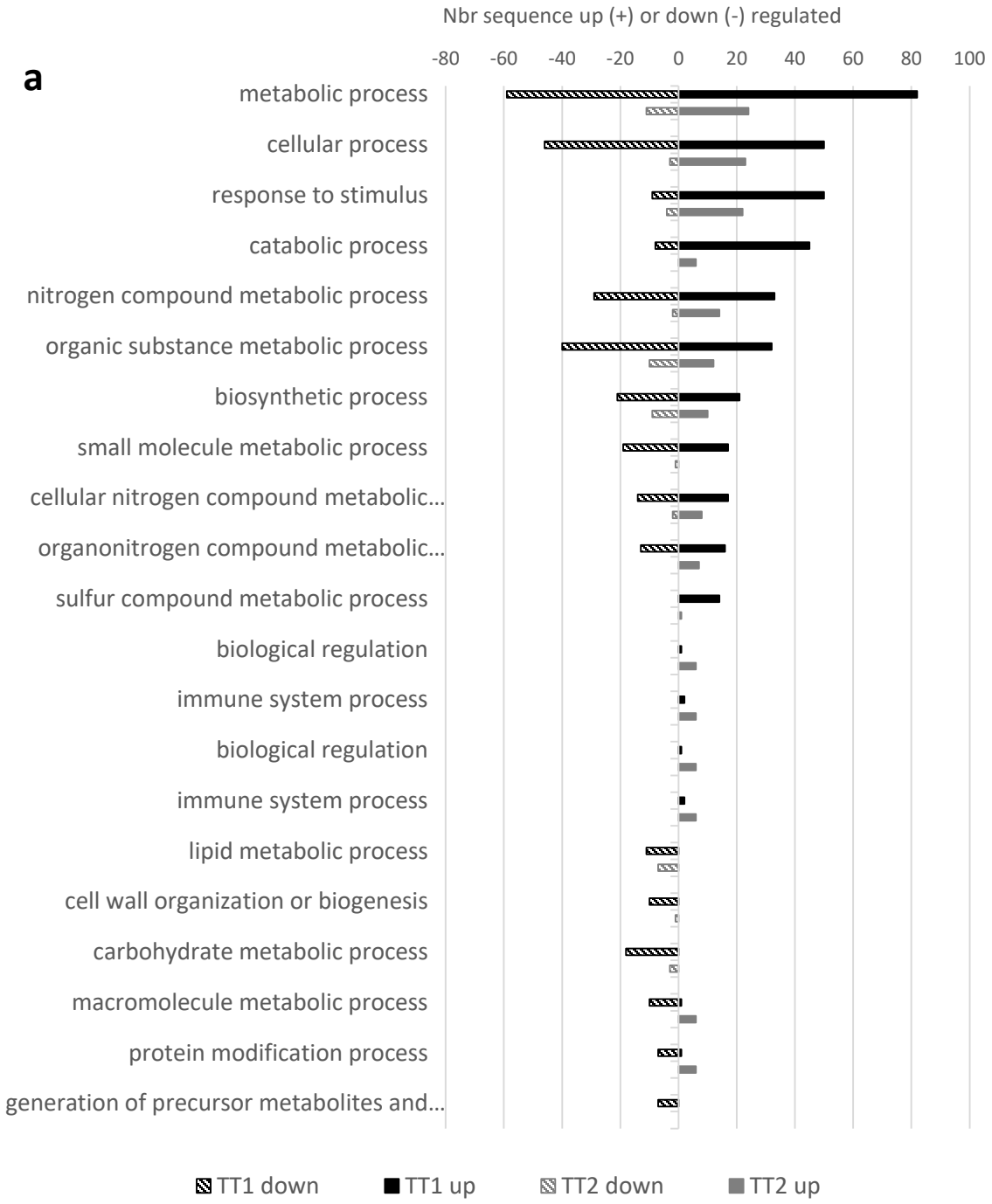

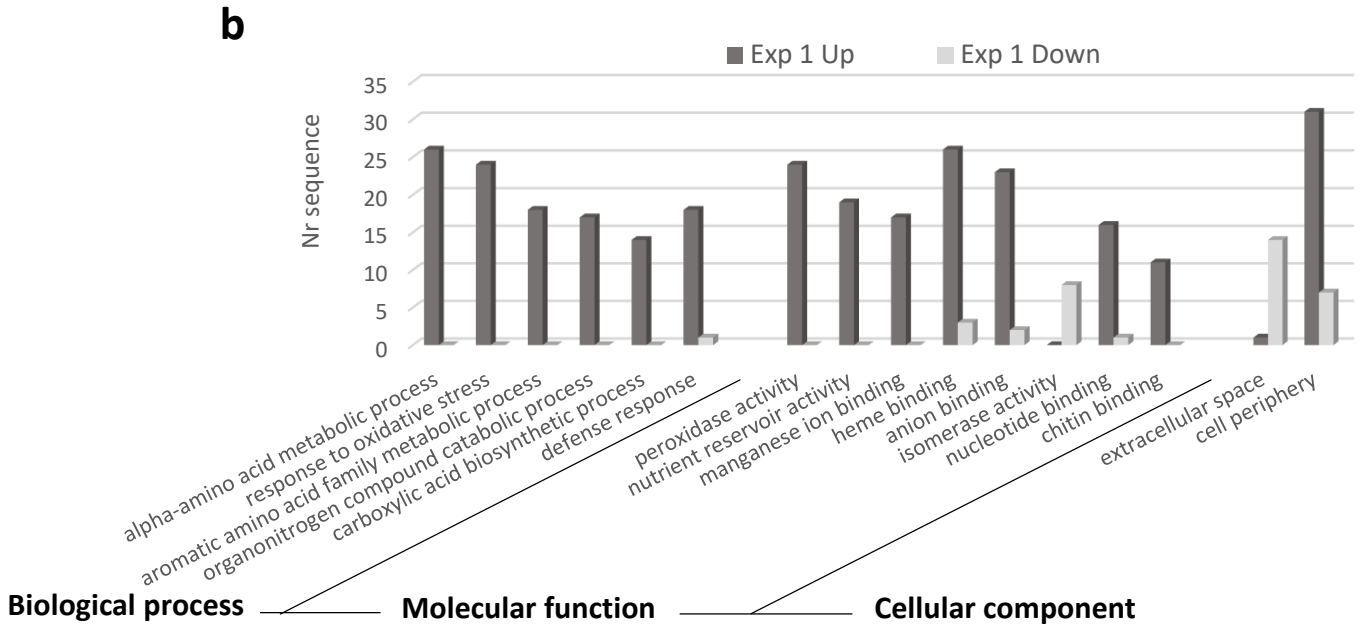

Fig. 1: Gene Ontology (GO) functional classification analysis. **a.** Distribution of annotated genes into functional categories according to GO biological process. **b.** GO functional classification analysis was made by comparing up and down-regulated genes found in Exp1 (Table S2) according to biological process, molecular function and cellular component through Fisher test. Number of sequences (Nr) were indicated for each category. BLAST2GO pipeline was used to get this GO annotation.

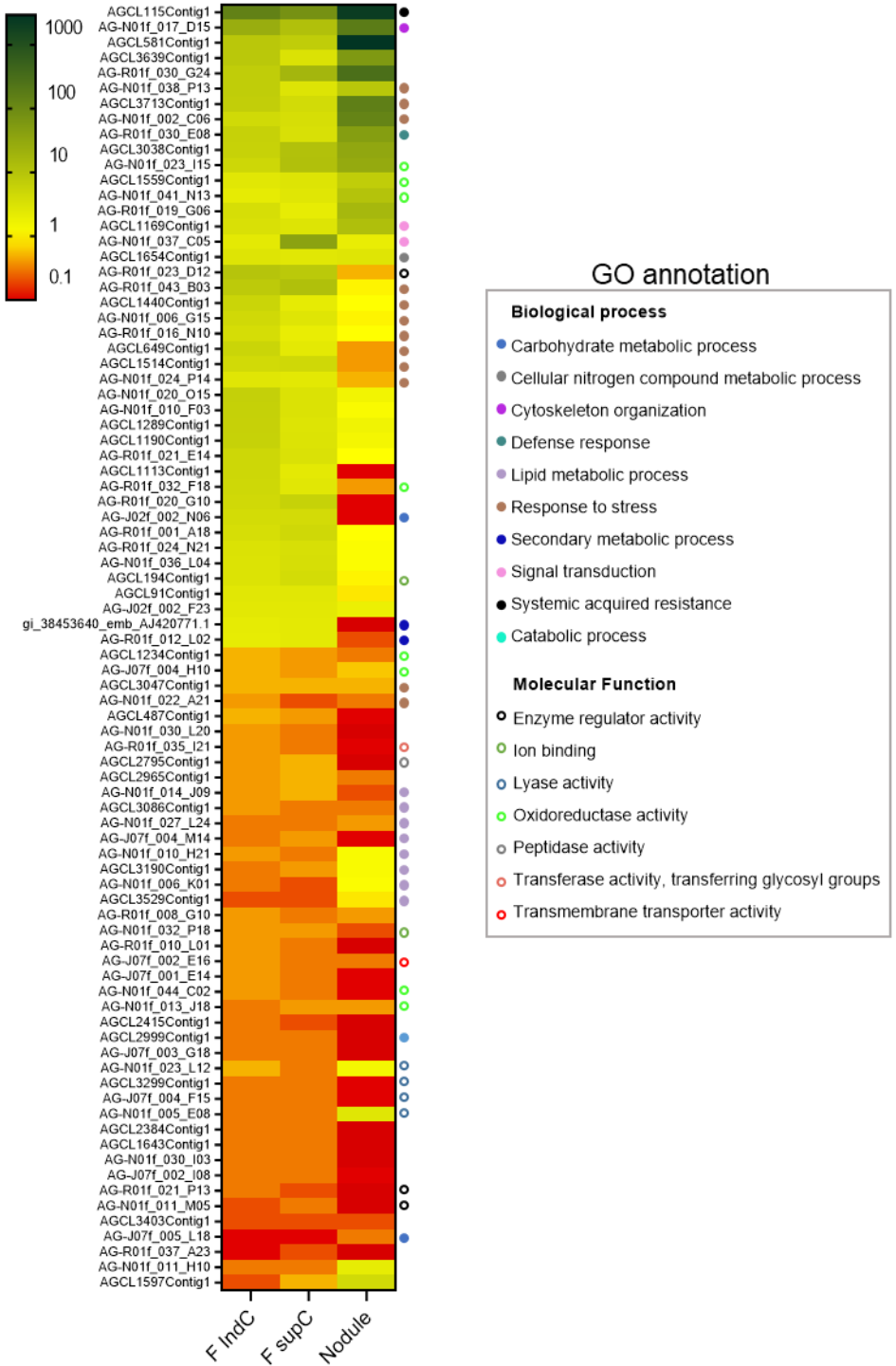

Fig. 2: Expression levels of the genes which were commonly upregulated and downregulated in *F*indC and *F*supC conditions. The expression level values in nodule were extracted from our previous work ((5); Table S4). The expression values were expressed as Fold change (FC) with a color gradient from red (down-regulated; ≤0.5) and orange-yellow (no-regulated) to green (up-regulated; ≥2) in infected roots or nodules compared to control roots without *Frankia*. The GO annotations were assigned by noting preferentially biological process and if not present, the molecular function. Certain genes have no GO assignation after blast2Go analysis. The heatmap was generated by GraphPad Prism 9.2.0.

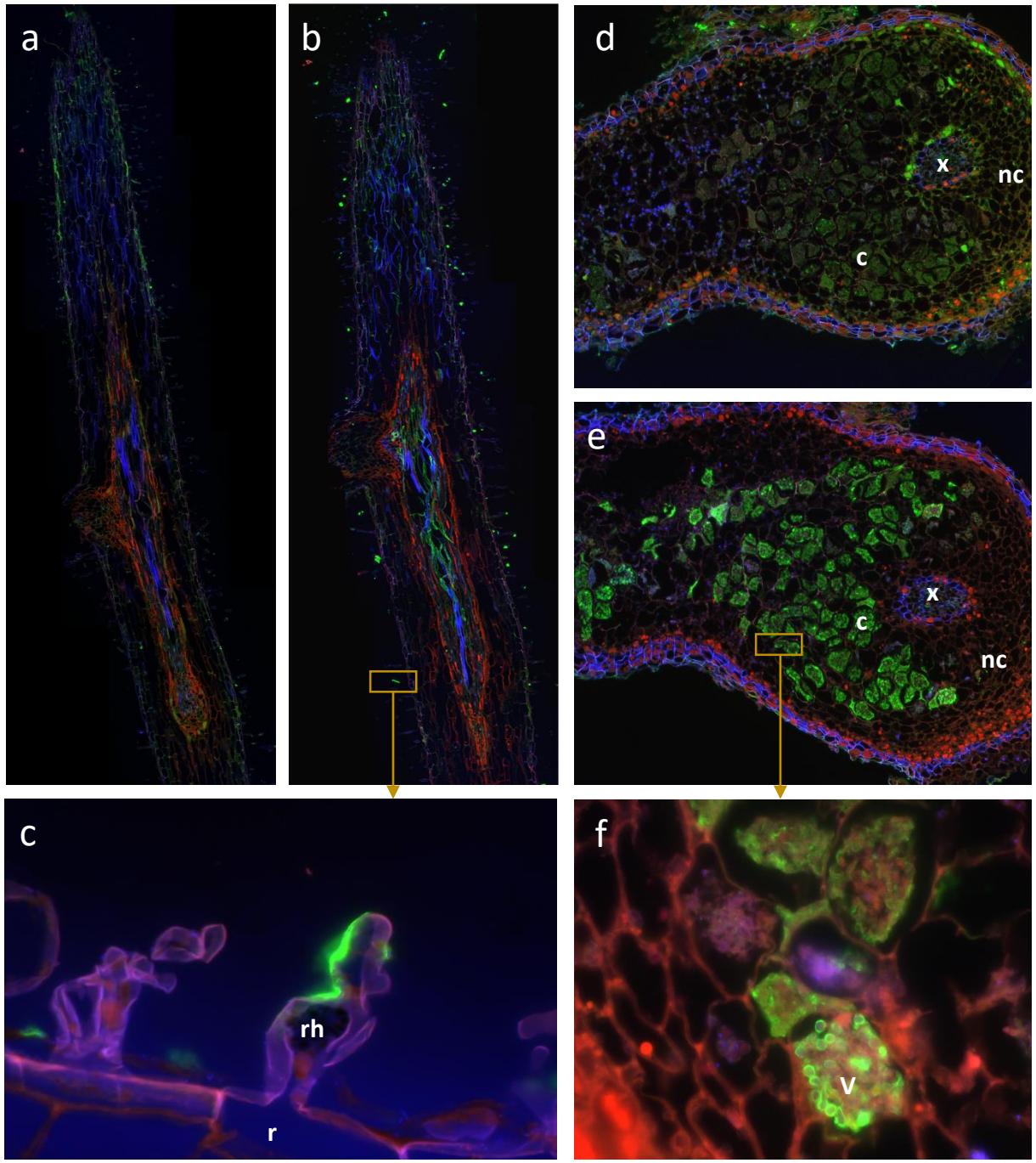

Fig. 3: **AgLTP24 localization in roots after 2.5 days (a, b, c) or nodule of 21 dpi (d, e, f).** Hair magnification of a specific zone of the infected root **(c)** or nodule **(f).** Immunofluorescence localization of AgLTP24 in hairy roots **(b, c)** and around *Frankia* vesicles in infected cells **(e, f)**. Negative control with rabbit serum before intramuscular injection of AgLTP24 epitope showed no green fluorescence in hairy roots **(a)** or infected cells **(d).** Blue: DAPI; red: autofluorescence; green: Alexa Fluor 488 dye anti-rabbit antibody (Life Technologies, Saint Aubin, France). c, infected cells; nc, noninfected cells; v, *Frankia* vesicles; x, xylem; rh, root hairs.

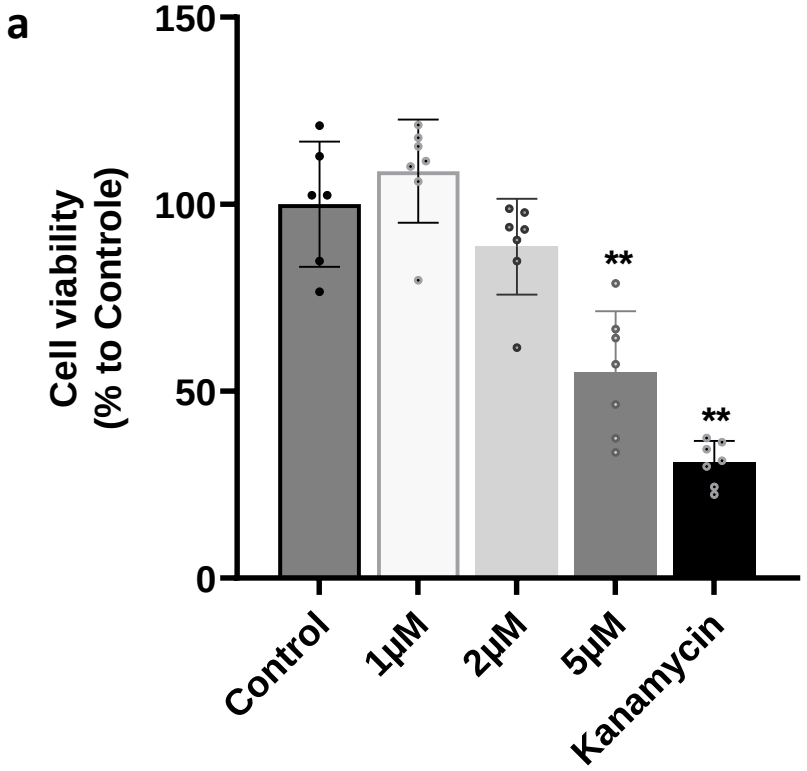

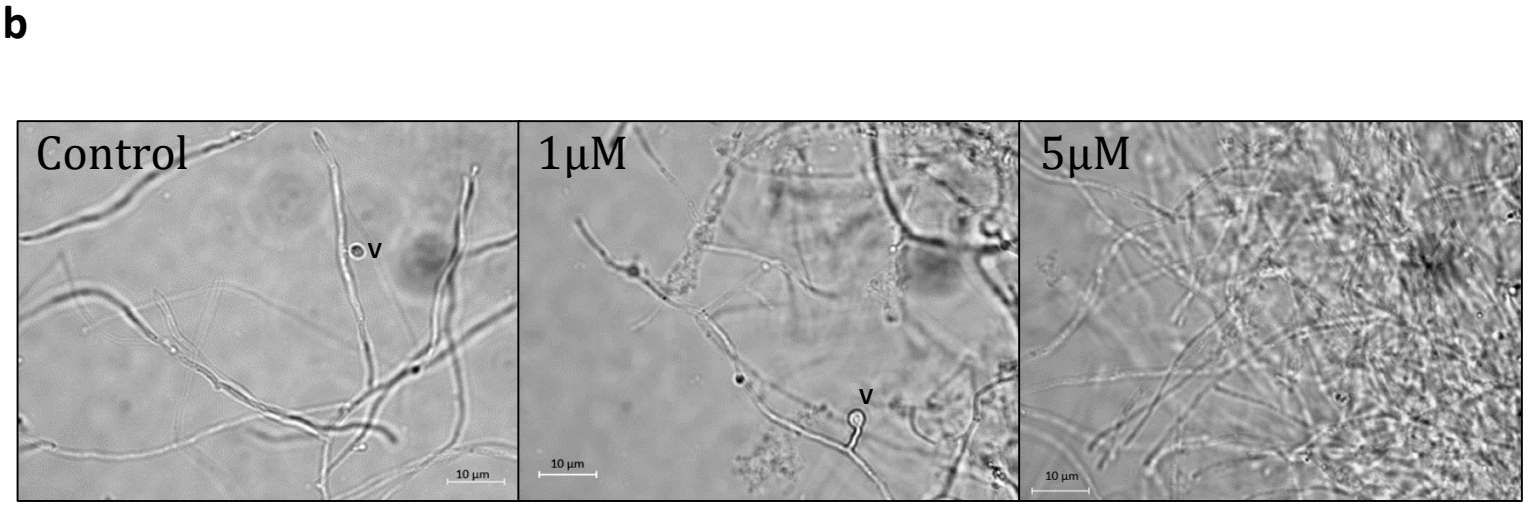

Fig. 4: physiological bioassays on *Frankia* growth and cellular development. **a.** Resazurin bioassay on *Frankia* ACN14a growth after supplementation of 1 to 5µM of AgLTP24. Cell viability was calculated by normalizing the fluorescence of the assay with the mean of the negative control (*Frankia* without AgLTP24). Kanamycin (40µg.ml^{-1}) was used as positive control. Data are expressed as mean values ± SD. Differences between normalized data were assessed by the Mann Whitney test (bilateral and unpaired) compared to control. Graphic representation and statistical analysis of results was conducted with GraphPad Prism version 9.2.0. *p value <0.05, **p value <0.01.
b. *Frankia* cells observation without or with gradual concentration of AgLTP24 from 0 (Control) to 5µM and obtained during the different physiological bioassays. v, *Frankia* vesicles

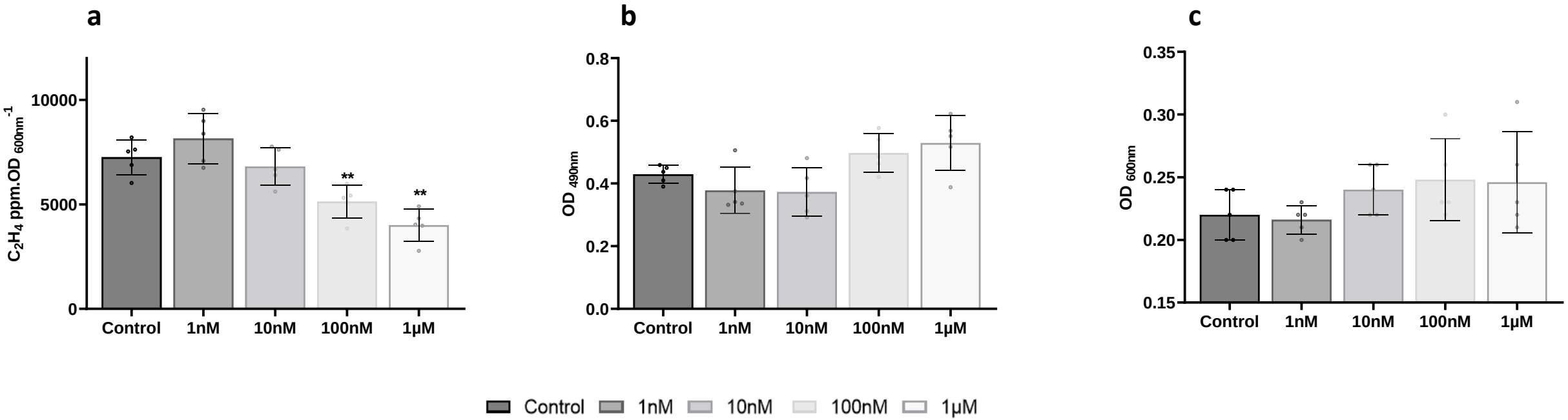

Fig. 5: effect of AgLTP24 in physiology of *Frankia* after 7 days of growth on **a.** Nitrogen fixation; **b.** respiratory activity and **c.** growth by measuring OD_{600nm}. Data were extracted from the kinetic assay (Fig. S5).
Data are expressed as mean values ± SD. Differences between means were assessed by the Mann Whitney test (bilateral and unpaired) compared to control. Graphic representation and statistical analysis of results was conducted with GraphPad Prism 9.2.0. *p value <0.05, **p value < 0.01.

Table 1: The up-regulated genes during early root hair deformation of *Alnus glutinosa* in both experiments, with *Frankia* indirect contact (*F* IndC) and with *Frankia* supernatant contact (*F* SupC)

For contigs, **EMBL-Accession** numbers of all the contigated EST sequences are indicated.

Singleton or contig **nucleotide sequences** are indicated when they were not of high-enough quality for EMBL submission acceptance.

Fold Change (**FC**) is the ratio between *F* IndC roots and control roots and between *F* SupC roots and control roots, respectively.

The significant difference of gene expression between *F* IndC roots and control roots and between *F* SupC roots and control roots (FC ≥ 2 or ≤ 0.05) was assessed by a T- test at p<0.05

*:Results of the previously reported microarray study with *Alnus glutinosa* nodules are indicated: **FC*** is the ratio between nodules and non inoculated root and **p*** is the p value of a T-student test comparing these two conditions (Hocher et al, 2011). ns indicated non significant difference between nodules and non inoculated root (p<0.05)

For EMBL-accession number, see Suppl Table 3.

** AGCL3038Contig1 sequence is the 3' non coding region of basic blue copper gene (AG-N01f_023_I15).

Clone Name	*Frankia* indirect contact (*F* indC)		*Frankia* supernatant contact (*F* supC)		Nodule[a]		Sequence homology	GO annotation	Peptide signal	Theoretical pI/Mw
	FC	p < 0.05	FC	p < 0.05	FC*	p*				
AGCL115Contig1	140.65	1.78E-06	74.8	1.12E-05	2145.65	1.38E-02	lipid transfer protein	systemic acquired resistance	Yes	8.46 / 9700.28
AG-N01f_017_D15	24.72	1.72E-06	11.7	2.09E-03	173.71	5.66E-03	betatubulin 14	microtubule-based process	No	ND
AG-R01f_023_D12	10.02	3.30E-04	8.4	3.79E-04	0.55	NS	pectin methylesterase inhibitor	pectinesterase inhibitor activity	Yes	4.41 / 16267.16
AGCL581Contig1	8.78	5.70E-04	7.1	4.17E-03	2941.04	7.08E-04	NA		0 Yes	10.07 / 11702.98*
AGCL3639Contig1	8.57	1.35E-05	3.1	1.66E-02	55.49	9.27E-03	NA		0 ?	ND
AG-R01f_043_B03	7.89	4.73E-04	12.0	6.70E-03	0.90	NS	Major pollen allergen Aln g 1	cellular response to stimulus	No	5.57 / 15622.87
AG-R01f_030_G24	7.07	4.26E-08	17.4	5.13E-04	288.39	4.27E-03	plant basic secretory protein (BSP), peptidase M		0 Yes	ND
AG-N01f_038_P13	7.06	3.27E-04	2.9	1.54E-02	9.13	1.52E-02	thaumatin like protein precursor		0 Yes	ND
AGCL3713Contig1	6.77	5.79E-03	4.1	1.27E-02	155.02	1.24E-03	defensin cysteine rich antimicrobial protein, Ag5 p	cellular response to stimulus	Yes	9.22 / 8145.27
AGCL1289Contig1	6.04	4.08E-08	2.9	2.15E-03	1.56	6.22E-03	proline-rich extensin-related protein-like		0 Yes	9.60 / 16039.35
AG-R01f_030_E08	6.04	4.68E-04	3.4	7.87E-03	46.10	1.19E-02	defensin cysteine rich antimicrobial protein, Ag11	cellular response to stimulus	Yes	7.01 / 6276.13
AGCL3038Contig1	5.67	4.96E-06	11.3	2.83E-04	31.43	4.86E-03	3' non coding region of basic blue copper gene		0 Non coding region	ND
AGCL649Contig1	5.21	1.80E-05	2.3	8.49E-03	0.43	3.64E-03	class III peroxidase	oxidation-reduction process	Yes	ND
AGCL1440Contig1	5.20	9.33E-06	2.2	2.81E-02	1.01	NS	chitinase / Hevein / PR-4 / Wheatwin2	cellular response to stimulus	Yes	5.01 / 18391.98
AGCL1113Contig1	4.71	1.92E-03	2.3	4.94E-02	0.14	2.92E-03	NA		0 Very small peptide	ND
AG-N01f_023_I15	4.71	5.29E-07	11.7	3.03E-05	28.29	4.31E-03	basic blue copper protein	oxidation-reduction process	Yes	9.82 / 10324.85
AG-R01f_032_F18	4.56	3.81E-06	2.5	1.20E-02	0.42	5.29E-03	cytochrome P450	oxidation-reduction process	Yes	ND
AG-R01f_020_G10	4.41	3.52E-07	5.9	9.86E-05	0.11	1.52E-02	germin like protein 5		0 Yes	ND
AG-N01f_006_G15	4.37	6.67E-07	2.7	4.29E-04	0.91	7.86E-02	cationic peroxidase	oxidation-reduction process	Yes	ND
AG-N01f_002_C06	4.34	6.70E-03	3.6	6.67E-03	125.38	7.39E-04	defensin cysteine rich antimicrobial protein, Ag3 p		0 Yes	9.36 / 6178.00
AGCL1514Contig1	4.19	1.79E-04	4.5	3.88E-03	0.36	4.66E-03	class IV chitinase	chitin catabolic process	Partial sequence	ND
AG-J02f_002_N06	3.88	9.15E-06	4.0	2.54E-02	0.06	1.41E-02	class V chitinase	carbohydrate metabolic process	Partial sequence	ND
AG-R01f_019_G06	3.64	2.46E-05	2.1	3.41E-02	16.08	1.32E-02	NA		0 ?	ND
AG-R01f_001_A18	3.59	3.12E-07	4.5	2.70E-03	1.03	NS	PRp27-like protein		0 Yes	6.10 / 23102.67
AGCL1169Contig1	3.29	4.34E-03	2.9	7.86E-03	12.42	2.83E-02	auxin-binding protein ABP20	cellular response to stimulus	Yes	ND
AG-R01f_024_N21	3.14	4.19E-06	3.5	4.05E-03	1.11	NS	PRp27 like protein		0 Partial sequence	ND
AG-N01f_036_L04	3.03	2.01E-05	3.6	1.09E-03	1.10	NS	PRp27 like protein		0 Partial sequence	ND
AGCL194Contig1	2.99	5.21E-05	3.9	9.30E-05	0.92	NS	germin like protein 5	cellular response to stimulus	Yes	6.07 / 21323.34
AGCL1654Contig1	2.81	2.39E-05	2.5	2.47E-02	2.70	1.03E-02	glutathione S-transferase		0 No	ND
AG-N01f_024_P14	2.56	1.89E-04	2.4	3.49E-02	0.45	1.20E-02	cationic peroxidase	oxidation-reduction process	Partial sequence	ND
AGCL91Contig1	2.50	4.18E-05	2.5	1.21E-02	0.83	NS	PRp27 like protein		0 Yes	5.79 / 23032.54
AGCL1559Contig1	2.45	8.83E-05	2.9	1.87E-02	7.18	2.70E-03	mannitol dehydrogenase	oxidation-reduction process	Partial sequence	ND
AG-J02f_002_F23	2.37	8.29E-06	2.4	4.34E-05	1.77	NS	NA		0 Small sequence	ND
AG-N01f_037_C05	2.26	9.10E-05	38.9	2.25E-05	1.97	6.01E-03	receptor protein kinase perk1 like protein	cellular response to stimulus	No	ND
AG-R01f_012_L02	2.12	1.18E-02	2.3	3.32E-03	0.22	3.61E-05	phenylalanine ammonia lyase		0 Partial sequence	ND
gi_38453640_emb_AJ420771.1	2.18	9.83E-03	2.31	3.66E-03	ND	ND	phenylalanine ammonia-lyase		No	ND